Metabolic Engineering 13 (2011) 588–597

Contents lists available at ScienceDirect

Metabolic Engineering

journal homepage: www.elsevier.com/locate/ymben

Optimization of a heterologous mevalonate pathway through the use of variant HMG-CoA reductases

Suzanne M. Ma [a,b], David E. Garcia [a,c,e], Alyssa M. Redding-Johanson [a,b], Gregory D. Friedland [a,d], Rossana Chan [a,b], Tanveer S. Batth [a,b], John R. Haliburton [a,b], Dylan Chivian [a,b], Jay D. Keasling [a,b,c], Christopher J. Petzold [a,b], Taek Soon Lee [a,b], Swapnil R. Chhabra [a,b,*]

[a] Joint BioEnergy Institute, Emeryville, CA, United States
[b] Physical Biosciences Division, Lawrence Berkeley National Laboratory, Berkeley, CA, United States
[c] Departments of Chemical Engineering and Bioengineering, University of California, Berkeley, CA, United States
[d] Biomass Science and Conversion Technology Department, Sandia National Laboratories, Livermore, CA, United States
[e] Department of Chemistry, University of California, Berkeley, CA, United States

ARTICLE INFO

Article history:
Received 6 May 2011
Received in revised form
30 June 2011
Accepted 13 July 2011
Available online 28 July 2011

Keywords:
Mevalonate pathway
Metabolic pathway optimization
HMG-CoA Reductase
E. coli
Cofactor regeneration
Mevalonate kinase

ABSTRACT

Expression of foreign pathways often results in suboptimal performance due to unintended factors such as introduction of toxic metabolites, cofactor imbalances or poor expression of pathway components. In this study we report a 120% improvement in the production of the isoprenoid-derived sesquiterpene, amorphadiene, produced by an engineered strain of *Escherichia coli* developed to express the native seven-gene mevalonate pathway from *Saccharomyces cerevisiae* (Martin et al. 2003). This substantial improvement was made by varying only a single component of the pathway (HMG-CoA reductase) and subsequent host optimization to improve cofactor availability. We characterized and tested five variant HMG-CoA reductases obtained from publicly available genome databases with differing kinetic properties and cofactor requirements. The results of our *in vitro* and *in vivo* analyses of these enzymes implicate substrate inhibition of mevalonate kinase as an important factor in optimization of the engineered mevalonate pathway. Consequently, the NADH-dependent HMG-CoA reductase from *Delftia acidovorans*, which appeared to have the optimal kinetic parameters to balance HMG-CoA levels below the cellular toxicity threshold of *E. coli* and those of mevalonate below inhibitory concentrations for mevalonate kinase, was identified as the best producer for amorphadiene (54% improvement over the native pathway enzyme, resulting in 2.5 mM or 520 mg/L of amorphadiene after 48 h). We further enhanced performance of the strain bearing the *D. acidovorans* HMG-CoA reductase by increasing the intracellular levels of its preferred cofactor (NADH) using a NAD^+-dependent formate dehydrogenase from *Candida boidinii*, along with formate supplementation. This resulted in an overall improvement of the system by 120% resulting in 3.5 mM or 700 mg/L amorphadiene after 48 h of fermentation. This comprehensive study incorporated analysis of several key parameters for metabolic design such as *in vitro* and *in vivo* kinetic performance of variant enzymes, intracellular levels of protein expression, in-pathway substrate inhibition and cofactor management to enable the observed improvements. These metrics may be applied to a broad range of heterologous pathways for improving the production of biologically derived compounds.

1. Introduction

Microbial production of desirable compounds through heterologous expression of foreign pathways commonly results in unintended consequences. Introduction of previously unknown and potentially toxic metabolites in the host organism may result in lower cell density and reduced product formation. Maintenance of a delicate balance between utilization of existing cellular resources for organism growth versus engineered manipulations such as enzyme overexpression is therefore an important aspect of metabolic optimization. Consequently, metabolic engineering strategies reported thus far have investigated accumulation of toxic intermediates (Berry et al., 2002; Pitera et al., 2007; Zhu et al., 2002), targeted improvements in protein production (Glick, 1995; Redding-Johanson et al., 2011), kinetics of rate limiting processes (Pfleger et al., 2006), spatial localization of key enzymatic activities (Chhabra and Keasling, 2011; Dueber et al., 2009; Pfleger et al., 2006; Zhang et al., 2008),

* Corresponding author at: Joint BioEnergy Institute, 5885 Hollis Street, Emeryville, CA 94608, United States. Fax: +1 510 486 4252.
E-mail address: srchhabra@lbl.gov (S.R. Chhabra).

1096-7176/$ - see front matter © 2011 Elsevier Inc. All rights reserved.
doi:10.1016/j.ymben.2011.07.001

and redox cofactor utilization by pathway components (Bennett and San, 2009; Berrios-Rivera et al., 2002; San et al., 2002).

The isoprenoid biosynthetic pathway is an important source of biopharmaceuticals, biochemicals, and advanced biofuels (Fortman et al., 2008). In nature, terpenoids are synthesized from the universal precursors isopentenyl pyrophosphate (IPP) and its isomer dimethylallyl pyrophosphate (DMAPP), which are generated either through the mevalonate (MEV) pathway or the deoxyxylulose 5-phosphate (DXP) pathway (Bochar et al., 1999; Hedl et al., 2004; Kuzuyama, 2002; Wilding et al., 2000). Generally, Gram-negative bacteria and eukaryotic organelles employ the DXP pathway, while humans, mammals, other eukaryotes, archaea and gram-positive cocci utilize the enzymes and intermediates of the mevalonate pathway (Bochar et al., 1999; Hedl et al., 2004). In *Escherichia coli* and other gram-negative bacteria, IPP and DMAPP generated from the natively regulated DXP pathway are essential metabolites for the prenylation of tRNAs and the synthesis of farnesyl pyrophosphate, which is central for quinone and cell wall biosynthesis (Connolly and Winkler, 1989). Enhanced sesquiterpene production in *E. coli* has been accomplished through the heterologous expression of the MEV pathway from *Saccharomyces cerevisiae* thereby bypassing the regulatory effects of its native DXP pathway (Harada and Misawa, 2009; Martin et al., 2003; Pitera et al., 2007). While this foreign MEV pathway is potentially unregulated in *E. coli*, its presence affects cellular behavior in significant ways. Notably, accumulation of the pathway intermediate 3-hydroxy-3-methylglutaryl-coenzyme A (HMG-CoA) has been shown to lead to bacteriostatic and bactericidal effects (Pitera et al., 2007). In addition, enzymatic conversion of HMG-CoA into mevalonate is the only redox cofactor utilization step in the entire MEV pathway and has the potential to disturb cellular redox balance (Berrios-Rivera et al., 2002; Heuser et al., 2007). The catalytic reaction performed at the HMG-CoA reductase step therefore represents a crucial bottleneck where metabolic engineering strategies may be applied to optimize the system for isoprenoid biosynthesis.

HMG-CoA reductase (HMGR), one of the few known four-electron oxidoreductases in nature, catalyzes the reduction of (*S*)-HMG-CoA to (*R*)-mevalonate (Fig. 1). Two moles of reduced pyridine nucleotide coenzyme are oxidized during the reduction of 2 mol of the thioester group of HMG-CoA to the primary hydroxyl group of mevalonate. HMGR is also able to catalyze the reverse reaction, the oxidative acylation of (*R*)-mevalonate to (*S*)-HMG-CoA. Based on sequence divergence, two classes of HMGRs have been proposed (Bischoff and Rodwell, 1992; Boucher et al., 2001; Istvan, 2001; Rodwell et al., 2000). Conventionally, class I HMGRs are typically found in higher organisms, generally prefer NADPH as the cofactor (Lawrence et al., 1995), and under physiological conditions, are effectively irreversible even though the enzymes catalyze the reaction in both directions *in vitro* (Bach et al., 1986; Lawrence et al., 1995; Sherban et al., 1985). In contrast, class II HMGRs comprise those from prokaryotes and archaea and generally prefer NADH as a cofactor (Kim et al., 2000; Theivagt et al., 2006).

It is well known that pathway optimization involves a complex interplay of factors such as: toxicity associated with newly introduced metabolites, disturbance in cellular redox state, *in vivo* enzymatic activity, and suboptimal protein expression levels. Previous efforts to alleviate the bottleneck at HMG-CoA reductase catalysis in microbial isoprenoid biosynthesis focused on manipulating features of only the native HMGR of the *S. cerevisiae* MEV pathway. These included modulation of enzyme production (Pitera et al., 2007), regulated enzyme production (Pfleger et al., 2006), and post-translational localization (Dueber et al., 2009; Zhang et al., 2008). The goal of this study was to alleviate the bottleneck associated with the HMG-CoA reduction step by perturbing enzymatic properties of HMGR while maintaining existing features of the engineered MEV pathway intact.

Our goal was to characterize enzymatic function in the context of a heterologous pathway expressed in an engineered host platform. We reasoned that direct assessment of such biochemical functionality would offer insight into the potential limitations of the engineered pathway and a rationale to resolve the corresponding bottlenecks. Here we exploited HMGR sequences from publicly available genome databases as a means to vary biochemical functionality of the reduction step while keeping the rest of the MEV pathway unchanged (Fig. 1). We investigated the kinetic characteristics of five HMGR variants individually as standalone enzymes and in the context of the entire MEV pathway to determine the ideal candidate for amorphadiene production. For the best performing HMGR variant, we further optimized amorphadiene production by improving preferred cofactor availability through the overexpression of a heterologous formate dehydrogenase. Our results emphasize the importance of

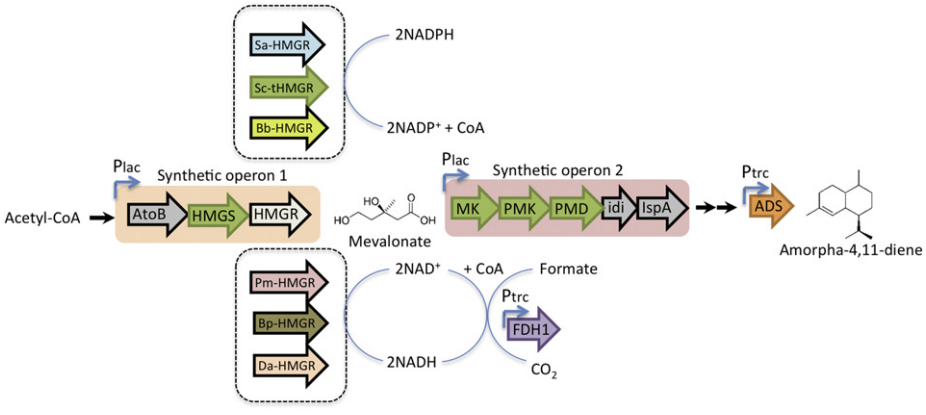

Fig. 1. Biosynthetic mevalonate pathway for isoprenoid production in *E. coli* towards amorpha-4,11-diene synthesis. Acetyl-CoA is diverted from central metabolism through the enzymes encoded in synthetic operon 1 to biosynthesize mevalonate. Synthetic operon 2 appropriates mevalonate to farnesyl pyrophosphate, which is subsequently extended to make the product, amorpha-4,11-diene. To increase intracellular pools of NADH the NAD^+-dependent formate dehydrogenase from *Candidia boidinii*, FDH yields a mole of NADH per mole of formate conversion to carbon dioxide. Genes originating from *E. coli* are colored in gray, genes originating from *S. cerevisiae* are in green, and the amorpha-4,11-diene synthase gene from *A. annua* is in orange. Organism abbreviations are as follows: *S. cerevisiae* (Sc), *P. mevalonii* (Pm), *S. aureus* (Sa), *B. petrii* (Bp), and *D. acidovorans* (Da). Gene abbreviations are as follows: acetoacetyl-CoA thiolase (*atoB*), HMG-CoA synthase (*HMGS*), HMG-CoA reductase (*HMGR*), mevalonate kinase (*erg12*, *MK*), phosphomevalonate kinase (*erg8*, *PMK*), phosphomevalonate decarboxylase (*MVD1*, *PMD*), IPP isomerase (*idi*), farnesyl diphosphate synthase (*ispA*), amorphadiene synthase (*ADS*), and formate dehydrogenase (*fdh1*).

investigating biochemical properties of individual pathway components in conjunction with protein expression in a non-native host, and the availability of essential cofactors for optimal production of reduced compounds such as advanced biofuels.

2. Material and methods

2.1. Bioinformatics analysis

The HMGR structures compared were those from *Pseudomonas mevalonii* (PDB id 1QAX) and human (PDB id 1DQA) and these were structurally aligned with PyMol (Delano WL. PyMol version 0.99). Multiple sequence alignments were built using MUSCLE (Edgar, 2004). The nearby sequences were added using BLAST against the non-redundant protein sequences database and using a conservative 40% minimum sequence identity cutoff and a maximum sequence identity cutoff of 90%.

2.2. Strains and media

E. coli strains DH10b and BLR(DE3), both from Invitrogen (Carlsbad, CA), were used for DNA manipulation, and protein overexpression, respectively. *E. coli* DH1 from ATCC (Manassas, VA) was used as the host for amorphadiene and mevalonate production. The pMevT plasmid bearing a chloramphenicol resistance marker contains the first three enzymes of the MEV pathway in synthetic operon 1 (Fig. 1) to convert acetyl-CoA (*atoB*) diverted from central metabolism to HMG-CoA (HMGS) to mevalonate (tHMGR). The pMBIS plasmid with a tetracycline resistance marker contains the genes in synthetic operon 2 (Fig. 1) to biosynthesize FPP from mevalonate. The pMBIS plasmid (Martin et al., 2003) possesses the *S. cerevisiae* genes mevalonate kinase (MK), phosphomevalonate kinase (PMK), and phosphomevalonate decarboxylase (PMD), and *E. coli* genes isopentenyl diphosphate isomerase (*idi*), and farnesyl diphosphate synthase (*ispA*). The pTrcADS plasmid harbors the amorpha-4,11-diene synthase (ADS) gene from *Artemisia annua* with an ampicillin resistance marker.

Components of the EZ-rich media kit used in all production experiments were purchased from Teknova (Hollister, CA). All chemicals were purchased from Sigma-Aldrich (St. Louis, MO). For all cloning, Phusion polymerase (New England Biolabs) was used for amplification, and for propagation of *E. coli*, Luria Broth with Miller's modifications (Sigma-Aldrich) was used with appropriate antibiotics for plasmid selection. Enzymes for molecular biology were purchased from Fermentas (Glen Burnie, MD).

2.3. Plasmid construction

All plasmids used are shown in Tables S1–S4. Using the pMevT plasmid (Martin et al., 2003) as a backbone, the original truncated 3-hydroxy-3-methyl-glytaryl-CoA reductase (tHMGR) from *S. cerevisiae* was exchanged with the HMGR from the following organisms: *Bordetella petrii*, *Delftia acidovorans*, *Pseudomonas mevalonii*, and *Staphylococcus aureus* (Fig. 1). Each HMG-CoA reductase gene was codon optimized for expression in *E. coli* and synthesized by GenScript Inc. (Piscataway, NJ). Standard molecular biology methods were used for construction of pMTDa, pMTBp, pSMA249 (see Supplemental Materials).

All standalone HMGRs were constructed using the following procedure and verified by protein quantification (data not shown). Each HMGR was amplified with the engineered restriction sites *NheI* and *EcoRI* flanking the gene and then gel purified. Each amplified HMGR and the pET24a(+) vector were subsequently digested (*NheI*/*EcoRI*), purified, and allowed to ligate to yield the final constructs listed in Table S1. Each HMGR was appended with a C-terminus His-tag for purification.

For anaerobic and aerobic mevalonate production experiments, the *E. coli lacI* gene was cloned into the plasmids: pMTDa, pMTBp, pMTSa, pMevT, and pMTPm. Primers in Table S4 were used in conjunction with splice by overlap extension PCR to place the *lacI* gene in each construct for controlled inducible expression.

To investigate the possibility of insufficient cofactor distribution during aerobic mevalonate and amorphadiene fermentation, the following two constructs were created. The *fdh1* formate dehydrogenase gene from *Candidia boidinii* was codon optimized and synthesized for expression in *E. coli* by GenScript Inc. (Piscataway, NJ). For standalone expression during mevalonate production, the gene was amplified with the primer pair shown in Table S3 with engineered restriction sites *EcoRI* and *BamHI* for placement into vector pBbE5a containing a P_{lacUV5} promoter, ampicillin resistance marker, and colE1 origin of replication to yield pSMa250. For expression *in cis* with the *A. annua* ADS gene, *fdh1* was amplified with engineered *BamHI*/*HindIII* flanking the gene and its own ribosome binding site (AAGGAGGATTACACT) precedes the gene. Resultant plasmid pSMa256 with genes *fdh1* and ADS expressed as one operon, but with individual ribosome binding sites, was used for amorphadiene production experiments.

2.4. Expression and purification of standalone HMGRs

All HMGR proteins were expressed and purified using the following procedure. The expression plasmids were transformed into *E. coli* BLR(DE3). The cells were grown at 37 °C in LB medium with 35 μg/mL kanamycin to an optical density of 0.4 at 600 nm. The cells were incubated on ice for 10 min and then induced with 0.1 mM isopropyl thio-β-D-galactoside (IPTG) for 16–24 h at 16 °C. Cells were harvested by centrifugation (5000 × **g**, Beckman Coulter Allegra 25 R, 10 min, 4 °C), and resuspended in 20 mM Tris–HCl, 10 mM imidazole, 500 mM NaCl, pH=7.9, lysed by sonication, and celluar debris was removed by centrifugation (10,000 × **g**, Beckman Coulter Allegra 25 R, 60 min, 4 °C). The supernatant was then put through a 0.4 μm filter prior to addition of Ni-nitrilotriacetic agarose resin (Qiagen) (2 mL/L culture). The proteins were allowed to interact with the resin at 4 °C for 1 h, and then each protein was purified using gravity flow affinity chromatography and eluted with increasing concentration of imidazole in the resuspension buffer. Purified proteins were concentrated and buffer exchanged into (50 mM Tris–HCl, 2 mM EDTA, 2 mM dithiothreitol, and 10% glycerol, pH=7.9), aliquoted, and flash frozen. Protein concentrations were approximated with the Bradford assay using BSA as a standard. Protein identity was confirmed and purity accessed by protein mass quantification.

2.5. Kinetic characterization of HMG-CoA reductase activities

Spectrophotometric assays of HMG-CoA reductase activity was performed on a SpectroMax Plus384 (molecular devices). All oxidation or reduction reactions following NADPH or NADH were monitored at 340 nm, with the reaction chamber maintained at 30 °C. Standard reaction conditions mimicked the intracellular conditions of the corresponding *in vivo E. coli* studies looking at amorphadiene or mevalonate production. Assays were conducted with a reaction temperature maintained at 30 °C and pH buffered to 7.9 in a final volume of 200 μl (Riondet et al., 1997). The assay following the forward reaction from (*S*)-HMG-CoA to (*R*)-mevalonate used 0.4 mM NAD(P)H as the cofactor, 0.30 mM (*R*,*S*)-HMG-CoA, 50 mM NaCl, 1 mM EDTA, 5 mM DTT, and 25 mM KH_2PO_4, pH 7.9 with an enzyme concentration of 0.3 mM. The reverse oxidative acylation of (*R*)-mevalonate to (*S*)-HMG-CoA was assayed with 50 mM $NAD(P)^+$, 5.0 mM Coenzyme A, 6.0 mM (*R*,*S*)-mevalonate, 50 mM NaCl, 1 mM

EDTA, 5 mM DTT, in 100 mM Tris–HCl, pH=7.9, and 0.3 mM enzyme. Reactions were first performed with mixtures containing enzyme plus all standard assay components except the initiating substrate to establish background states. Reactions were initiated by the addition of HMG-CoA or mevalonate. Specific activity is defined as μmol/min/mg-protein (Units/mg P), one enzyme unit represents the turnover, in 1 min, of 1 μmol of nicotinamide nucleotide coenzyme at 30 °C. Reported data are mean values for at least triplicate assays.

2.6. Kinetic characterization of mevalonate kinase

All chemicals and enzymes were purchased from Sigma-Aldrich. *S. cerevisiae* mevalonate kinase (MK), was a gift from Amyris Biotechnologies. All non-enzyme solutions were 0.2 μM filter-sterilized (P.N. 190-2520, Thermo Scientific). ATP stocks were adjusted to pH = 7.0 with tris-base. The extinction coefficients of ATP ($15.4\ mM^{-1}\ cm^{-1}$ at 259 nm) and NADH ($6.22\ mM^{-1}\ cm^{-1}$ at 339 nm) were used to determine stock concentrations. Mevalonate was made by the saponification of mevalonolactone with KOH at 1.5:1 (mol:mol) KOH:mevalonolactone for 2 h at 37 °C, 200 rpm. Conversion was verified via normal phase TLC, developed in isopropanol and stained with basic permanganate. Mevalonate stocks were titrated to pH=7.0. 1 mL enzymatic assay mixtures contained: 200 mM Tris–HCl (pH=7.0), 100 mM KCl, 6 mM $MgCl_2$, 0.24 mM NADH, 3.0 mM ATP, 1.0 mM PEP, 0.5–50 mM mevalonate, 6.82 U pyruvate kinase, 9.90 U lactate dehydrogenase, and 1 μg MK. Reactions progress at 30 °C and were monitored spectrophotometrically at 339 nm for NADH consumption. Triplicate reactions were performed for statistical analysis, from which average reaction velocities were calculated in μM product formed per minute per μg MK added.

2.7. Aerobic growth conditions for mevalonate analysis

For kinetic characterization of each HMGR variant physiologically, each HMGR variant in synthetic operon 1 was transformed into *E. coli* DH1 for mevalonate analysis. An overnight inoculum was grown at 37 °C in 10 mL of LB medium containing chloramphenicol (30 μg/L). Baffled flasks containing 50 ml EZ-Rich Media supplemented with 1% glucose and antibiotic were inoculated to an OD_{600} of 0.1 and induced immediately with 500 mM IPTG. OD_{600} and mevalonate production were assayed at 24, 48, and 72 h post induction. Optical densities of samples were taken from cultures and measured using a UV–vis spectrophotometer (Beckman, Fullerton, CA). Mevalonate concentrations were extracted, analyzed, and determined (see Supplemental Materials).

2.8. Aerobic growth conditions for amorpha-4,11-diene analysis

To determine the effectiveness of each HMGR variant on overall amorpha-4,11-diene production, each HMGR variant was assayed by triple transformation of *E. coli* DH1 with synthetic operons 1 and 2 and the pTrcADS plasmid (Anthony et al., 2009). Overnight inoculums were grown in 10 mL LB medium with chloramphenicol (30 μg/L), ampicillin (50 μg/L), and tetracycline (12.5 μg/L) at 37 °C. All production experiments followed an analogous inoculation scheme as for mevalonate experiments. Induction was carried out at mid-log phase $OD_{600}\sim0.4$ with 500 mM IPTG and the addition of a 20% (v/v) dodecane (Sigma-Aldrich) overlay to capture the volatile product (Newman et al., 2006). Incubation temperature, OD_{600}, and amorpha-4,11-diene production time points were the same as for mevalonate experiments. Amorphadiene concentrations were determined by GC-MS analysis (see Supplemental Materials).

2.9. Aerobic growth conditions for amorpha-4.11-diene analysis with FDH

Plasmids pSMa256, pMTDa, and pMBIS were co-transformed into electrocompetent *E. coli* DH1. Overnight inoculum was grown as in aerobic mevalonate production experiments. Production experiments were performed identically to those not expressing the *fdh1* gene, except for the addition of exogenous formate 2 h post induction. Organic extraction and OD_{600} measurements were performed as described above.

2.10. Anaerobic growth conditions for mevalonate and amorpha-4,11-diene analysis

Optical density measurements for all time points were measured as with aerobic experiments. The majority of sample handling was carried out in an anaerobic glove box (Coy Laboratory Products, Inc., Grass Lake, MI) with a nominal gas composition of 85% N_2–10% CO_2–5% H_2. Clean and sterile serum bottles, rubber bottle caps, metal seals, and all plasticware were put into the anaerobic glove box for a minimum of 16 h prior to use. Anaerobic water was prepared by autoclaving to sterilize and then purging with filtered nitrogen (for both oil and microbes) for 2–3 h concurrent with cooling. Anaerobic medium was prepared by allowing EZ-Rich medium to equilibrate in the anaerobic glove box for at least 6 h before mixing with anaerobic water. Initial cell cultures were started in 10 mL culture tubes aerobically and allowed to grow overnight (37 °C, 200 rpm). For mevalonate and amorphadiene production experiments the overnight inoculum was taken into the anaerobic chamber and diluted to an OD_{600} of 0.1 in a total volume of 50 ml of EZ-Rich medium with 1% glucose and antibiotics. Sealed serum bottles were removed from the chamber and allowed to adapt to the anaerobic environment on a shaking platform (Kuhner) overnight. After 12–16 h of anaerobic adaptation serum bottles were opened anaerobically and a volume of cell culture was taken to yield the cellular density of 0.1 in the production cultures and pelleted in 50 mL falcon tubes ($7000\times\mathbf{g}$, 5 min). The pelleted cells were taken into the anaerobic chamber where the supernatant was discarded and the cells resuspended in anaerobic medium containing antibiotics and 0.1 mM IPTG for induction. Aliquots (50 mL) of cell culture were distributed in triplicate into clean serum bottles, which were capped and sealed. For intermediate time points the bottles were opened in the anaerobic chamber, sampled, and resealed. For amorphadiene production, 20% (v/v) dodecane was added to capture the volatile sesquiterpene. Mevalonate and amorphadiene extraction and quantification were performed as in aerobic experiments.

2.11. Proteomics sample preparation and analysis

For proteomic analysis, cells were prepared and treated as reported previously by (Redding-Johanson et al., 2011) (see Supplemental Materials).

2.12. Proteomics peak area determination

MultiQuant 1.2™ software (Applied Biosystems) was used to determine the peak area for all MRM transitions. Automatic peak integration using the Intelliquant algorithm was used with peak smoothing set to 3. As three to four transitions were selected for every protein, peak areas were summed for each protein to yield a total peak area. Absolute intensities between samples cannot be directly compared due to differences in instrument and column performance. Consequently, total peak area for each protein was normalized to the total peak area of the internal standard,

chloramphenicol to give a normalized total peak area for each protein. This normalized total peak area was averaged for three replicate analyses, and the standard deviation was calculated.

3. Results and discussion

3.1. Target gene selection

To explore the innate flexibility of replacing the tHMGR from *S. cerevisiae* with suitable homologs, we examined existing sequence databases for known or predicted HMGRs. To aid in the breadth of coverage we chose two well-characterized representative HMGRs as templates: one from prokaryotic class II and another one from eukaryotic class I. We examined structural information for the class II NADH-dependent HMGR from *P. mevalonii*, and compared it to the class I NADPH-dependent human HMGR. Superimposition of the *P. mevalonii* and human HMGR structures showed similar active site architectures with 1.1 Å root mean squared deviation of residues with side-chain atoms within 5 Å of the cofactor (Fig. S1). Close comparison of the two proteins structures revealed a key aspartate (D646) residue in the *P. mevalonii* HMGR that could potentially contribute to cofactor specificity (Bensch and Rodwell, 1970; Gill et al., 1985; Jordan-Starck and Rodwell, 1989). We postulated that the negatively charged aspartate repels the negatively charged phosphate in NADPH, resulting in a strong preference for NADH. We investigated the role of this residue in cofactor specificity for other mesophilic bacterial HMGR sequences by building a multiple sequence alignment of eight class II HMGRs from: *Delftia acidovorans*, *Bordetella petrii*, *P. mevalonii*, *Staphylococcus aureus*, *Borrelia burgdorferi*, *Archaeoglobus fulgidus*, *Listeria monocytogenes*, *Streptomyces sp.* strain CL190, and one class I HMGR from *S. cerevisiae*. The sequence alignments revealed that *D. acidovorans*, *B. petrii*, and *A. fulgidus* all possess an aspartate at position 646, while the other selected HMGRs did not. To statistically evaluate the importance of the specificity-determining residue, we constructed a multiple sequence alignment of 98 additional HMGRs. The selected HMGRs varied in sequence identity (40–90%) relative to the eight variants described above. The resulting distribution of amino acids at position 646 strongly favors aspartate in sequences similar to the NADH-binders (*P. mevalonii* and *A. fulgidus*) and has very few aspartates at this position in NADPH-binders or HMGRs with dual-cofactor specificity (*S. cerevisiae*, *S. aureus*, *S. sp.* strain CL190, and *L. monocytogenes*) (Fig. 2). Based on these results, we picked a set of NADH-preferring (from *D. acidovorans*, *B. petrii*, and *P. mevalonii*) and NADPH-preferring (from *S. aureus* and *S. cerevisiae*) HMGR variants.

3.2. In vitro HMG-CoA reductase characterization

We first investigated each homolog as a standalone enzyme decoupled from the MEV pathway. We proceeded to construct expression vectors for each HMGR variant by designing the corresponding gene sequences for optimal expression in *E. coli* (see the section Methods). All pET24a-derived expression vectors listed in Table S1 were transformed into *E. coli* BLR (DE3) individually and purified by nickel affinity chromatography. We conducted enzyme assays to determine the ability of each HMGR variant to catalyze the forward reductive deacylation of the thioester group of HMG-CoA to the primary alcohol of mevalonate as well as the reverse oxidative acylation of mevalonate to HMG-CoA. Kinetic assays were monitored at 340 nm following the use of NAD(P)H as a co-substrate for the forward reaction, and the formation of a co-substrate from $NAD(P)^+$ for the reverse reaction (Fig. 3). To mimic the expected intracellular environment of *E. coli* we maintained the reaction pH at 7.9, and selected the production temperature, 30 °C.

The kinetic capabilities of each HMGR variant under a controlled *in vitro* environment are shown in Fig. 3. Experimentally determined cofactor preferences matched well with our computational predictions described above lending credence to the possible role of the aspartate at position 646 (Rodwell et al., 2000). Among the five HMGRs tested in this study, the NADPH-dependent *S. aureus* enzyme exhibited the highest forward reaction rate of 11.42 ± 1.55 eU/mg P, which was 5-fold greater than its reverse reaction (2.34 ± 0.13 eU/mg P). In contrast to its prokaryotic counterparts the class I HMGR from *S. cerevisiae* exhibited an insignificant reverse reaction rate (0.43 ± 0.01 eU/mg P), distinctive of eukaryotic HMGRs (Bach et al., 1986; Lawrence et al., 1995; Sherban et al., 1985). Scrutiny of

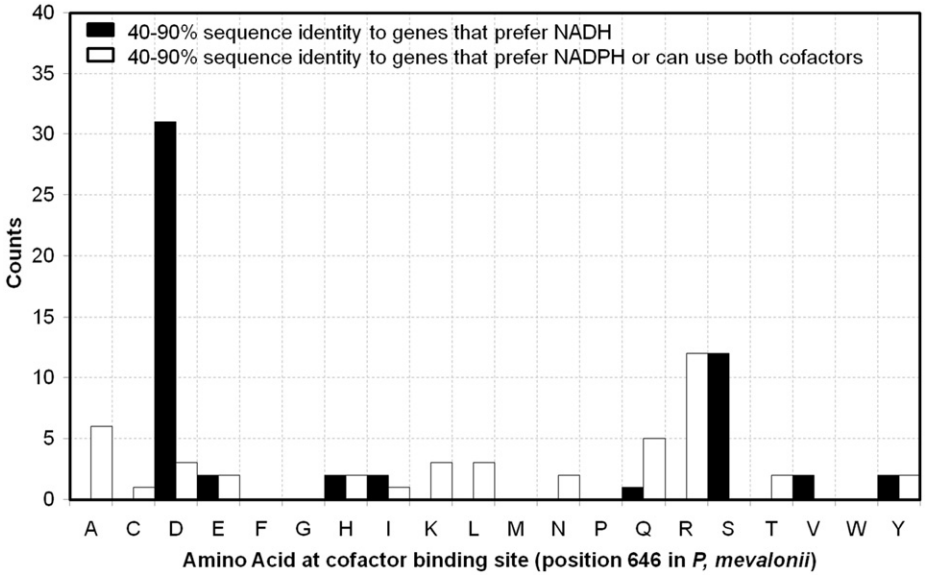

Fig. 2. Distribution of amino acids at the specificity-determining position of HMGRs (D646 from *Pseudomonas mevalonii*) from an alignment of 98 HMG-CoA reductase sequences (HMGRs). The sequences were found based on similarity to experimentally-characterized HMGRs (Beach and Rodwell, 1989; Boucher et al., 2001; Takahashi et al., 1999; Theivagt et al., 2006; Wilding et al., 2000).

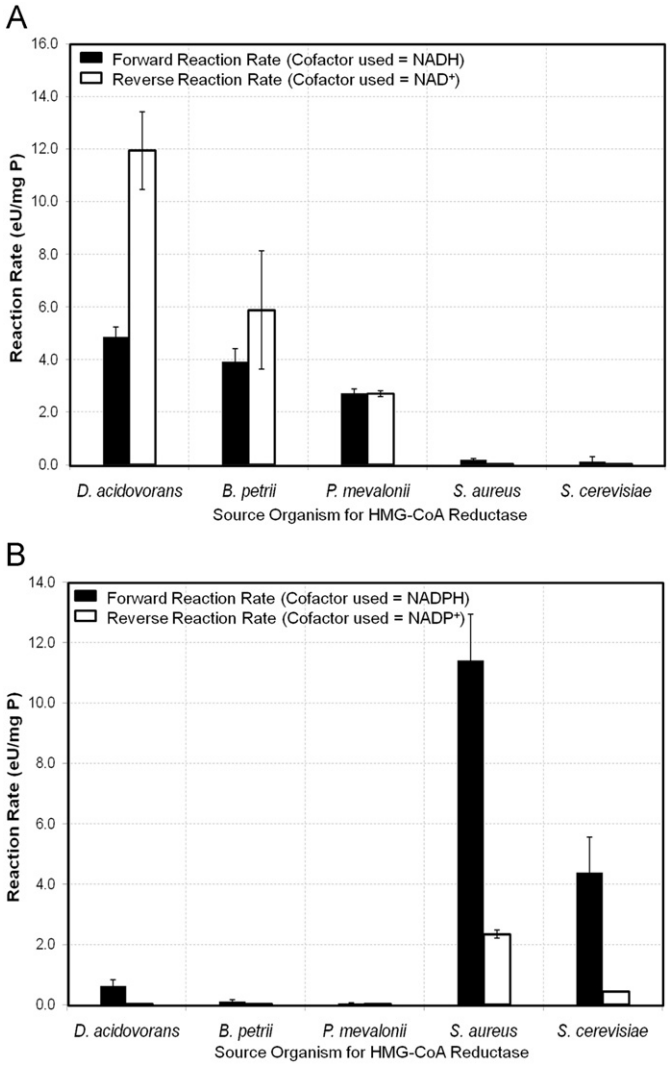

Fig. 3. *In* vitro catalytic comparison of HMG-CoA reductases expressed and purified from *E. coli*. Kinetic characterization of forward reductive deacylation of HMG-CoA to mevalonate (black) and reverse oxidative acylation to HMG-CoA (white). (A) Kinetic reactions containing only NADH as the cofactor. (B) Kinetic reactions containing only NADPH as the cofactor. All HMGRs displayed stringent cofactor specificity. All bacterial HMGRs displayed forward and reverse kinetics. The eukaryotic HMGR did not exhibit appreciable reaction in the reverse direction beyond the margin of error. eU/mg P, enzyme unites per milligram of protein.

the NADH-preferring HMGRs (from *B. petrii*, *D. acidovorans*, and *P. mevalonii*) showed that these prokaryotic HMGRs were able to process the reverse reaction to appreciable extents. Notably, the enzyme from *P. mevalonii* catalyzed the forward (2.73 ± 0.17 eU/mg P) and reverse reactions (2.70 ± 0.12 eU/mg P) equally effectively, a characteristic indicative of the host organism's ability to utilize mevalonate as the sole carbon source for growth (Takahashi et al., 1999). Interestingly, the two new HMGRs that identify most closely with the *P. mevalonii* HMGR in terms of sequence identity exhibit the same inclination towards an appreciable reverse reaction. The HMGR from *D. acidovorans* had the highest reverse reaction rate (11.94 ± 1.48 eU/mg P), which was 2.5-fold faster than the corresponding forward reaction (4.87 ± 0.38 eU/mg P). The HMGR from *B. petrii* appeared to possess kinetic characteristics between those observed for its counterparts from *P. mevalonii* and *D. acidovorans*. While *in vitro* studies offer a good indication of cofactor preference and kinetic capabilities, enzymatic performance in a foreign host is a function of additional factors such as intracellular protein levels and host cofactor availability, both of which can equally impact the effective enzymatic activity under the chosen growth conditions.

3.3. *In vivo* HMGR characterization: protein quantification and mevalonate production

Next we examined *in vivo* characteristics of each HMGR with regard to mevalonate production. Each HMGR variant was cloned in place of the *S. cerevisiae* tHMGR in synthetic operon 1 (Fig. 1). Plasmids in Table S4 as well as the original construct containing the *S. cerevisiae* tHMGR were transformed into the sesquiterpene. production strain, *E. coli* DH1. Apart from the HMG-CoA reductase, all other components of the pathway remained unchanged, allowing us to directly compare the contribution of each HMGR towards mevalonate production. Cell density and protein quantification measurements taken at 24, 48, and 72 h post induction revealed nearly no changes in growth 24 h post induction (data not shown). In contrast, mevalonate production continued to increase until 48 h after induction, but remained nearly steady thereafter (Fig. S3). Consequently, we chose to compare *in vivo* performance of the variant enzymes at 48 h post induction given the attainment of *in vivo* equilibrium. We assayed individual HMGR performance during *in vivo* aerobic and anaerobic fermentation. We determined intracellular mevalonate production by organic extraction followed by GC-MS analysis, and protein abundances using proteomic techniques (see Sections 2.11 and 2.12). While protein abundance levels varied widely between different HMGRs during aerobic fermentation, the observed mevalonate levels seemed to reflect the *in vitro* kinetic behavior described above to a large extent (Fig. 4). In the absence of the remaining components of the mevalonate pathway on synthetic operon 2 as well as the amorphadiene synthase, the mevalonate levels represent equilibrium values as a result of the forward and reverse reactions. Notably, the HMGR from *S. aureus*, which was observed to have the greatest forward reaction rate coupled with a low reverse reaction rate, yielded the highest level of mevalonate (2.85 mM). HMGRs from *S. cerevisiae* and *B. petrii* produced comparable levels of mevalonate (2.34 and 2.33 mM, respectively). It is likely that the comparable levels of mevalonate accumulated for the strains bearing the

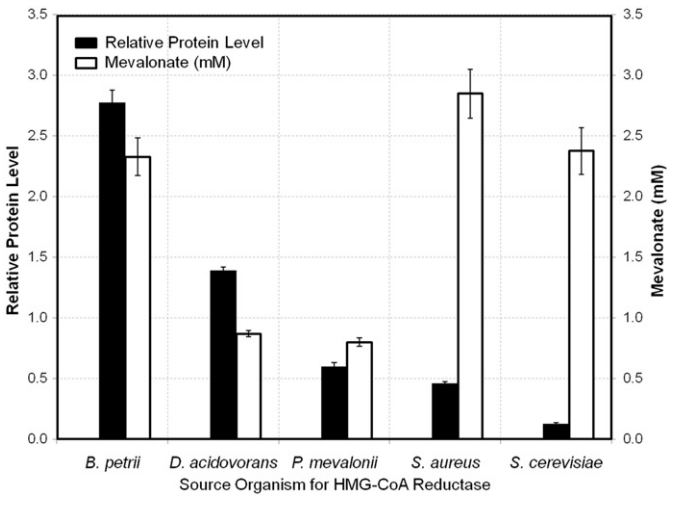

Fig. 4. *In vivo* aerobic mevalonate production (black) in relation to relative protein expression levels (white). Induced expression of the first synthetic operon in *E. coli* DH1, grown in EZ-rich medium supplemented with 1% glucose at 30 °C. Cell cultures were induced at induction with 0.5 mM IPTG. Mevalonate was extracted 48 h after induction and examined by GC–MS. All cultures reached a similar cell density approximately $OD_{600} \approx 5$. Protein levels are normalized to chloramphenicol concentrations. Results are the average of three technical replicates with error bars showing the standard deviation from the mean value.

S. cerevisiae and *B. petrii* enzymes are a function of both enzyme kinetics and *in vivo* protein expression levels (Figs. 3 and 4). The largest contribution to mevalonate accumulation by the *S. cerevisiae* enzyme may be attributed to the fact that it lacks the ability to perform the reverse reaction. However, the sizeable amount of mevalonate produced by the *B. petrii* enzyme, considering it has similar kinetic properties to the *D. acidovorans* and *P. mevalonii* enzymes, is most likely ascribed to the abundance of this protein. *In vivo* protein quantification studies show that the *B. petrii* enzyme expressed almost 3-fold more abundantly than the corresponding enzymes from *D. acidovorans* and *P. mevalonii*. It appears that for these enzymes to compensate for slower kinetics, protein abundance must be greater than 3-fold to produce the same amount of mevalonate as those enzymes with high forward reaction rates and low reverse reaction rates.

Critical examination of mevalonate production under aerobic and anaerobic growth conditions highlights the segregation between the variant HMGRs in terms of their cofactor specificities. Variant HMGRs that preferred NADH as a cofactor (*B. petrii, D. acidovorans,* and *P. mevalonii*) produced less mevalonate than those that required NADPH (*S. cerevisiae* and *S. aureus*) during aerobic growth (Fig. 4). During anaerobic growth the NADH-preferring enzymes produced greater levels of mevalonate than their NADPH-dependent counterparts (Fig. S4). These findings were not unanticipated, given that the intracellular metabolite concentrations of NADH found in *E. coli* during aerobic growth are less than those of NADPH with the reverse trend being observed under anaerobic conditions (Bennett and San, 2009; Leonardo et al., 1996).

3.4. Improvement in amorpha-4,11-diene production with variant HMGRs

To determine the effects of HMGR perturbation on the entire mevalonate pathway, we created strains harboring synthetic operon 1 with variant HMGRs, the plasmid bearing synthetic operon 2, and the plasmid including the amorpha-4,11-diene synthase gene. While we anticipated a direct correlation between mevalonate and amorphadiene production levels given that the pathway post-HMGR was identical in each strain and none of the additional pathway enzymes are cofactor dependent, we observed significant inconsistencies across the various strains. The *S. aureus* and *S. cerevisiae* enzymes produced the most mevalonate, but did not produce the most amorphadiene (Fig. 5). Surprisingly, the *D. acidovorans* HMGR, which produced the lowest amount of mevalonate, generated the most amorphadiene; even outperforming the *B. petrii* enzyme, which had a 3-fold advantage in protein quantity and an almost 2-fold advantage in mevalonate production. The disparity in amorphadiene production could not be attributed to cell density, given the relatively comparable cell densities of each variant (Fig. S5). One possibility that might contribute to this apparent inconsistency between the mevalonate and amorphadiene levels of variant HMGRs, could be the kinetic properties associated with the enzyme that mediates the next step of the engineered pathway—mevalonate kinase (MK).

3.5. Substrate inhibition of the mevalonate kinase from S. cerevisiae

We measured the initial reaction rates of the *S. cerevisiae* mevalonate kinase under ATP saturating conditions with increasing levels of mevalonate and found that the fastest average reaction rate was observed around 2.5 mM mevalonate (Fig. 6). At mevalonate concentrations greater than this the reaction rate of *S. cerevisiae* MK begins to decrease. Substrate inhibition at high mevalonate concentrations has also been reported previously for the MK from *S. aureus* (Voynova et al., 2004).

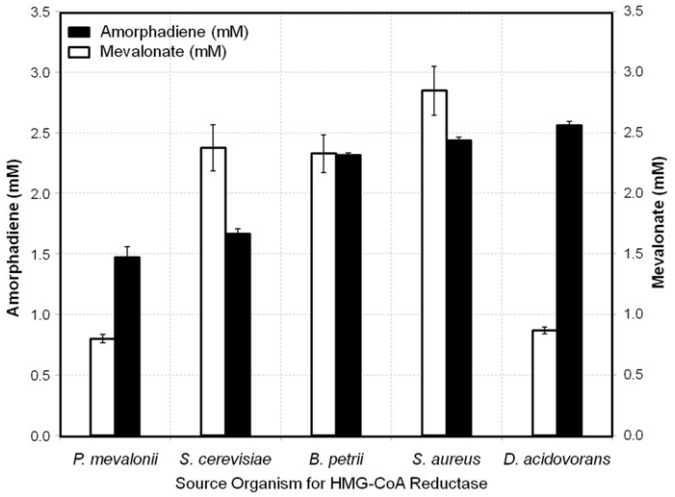

Fig. 5. *In vivo* aerobic production of amorphadiene (black) in relation to mevalonate (white). Mevalonate production was measured as before. The plasmids bearing synthetic operon 1, synthetic operon 2, and the amorphadiene synthase were co-expressed in *E. coli* DH1, grown in EZ-rich medium supplemented with 1% glucose at 30 °C. Cell cultures were induced with 0.5mM IPTG at mid-log phase, $OD_{600}\sim 0.4$. Amorphadiene and mevalonate levels were examined by GC-MS following organic extraction 48 h after induction. All cultures reached a similar cell density approximately $OD_{600}\approx 5$. Results are the average of three technical replicates with error bars showing the standard deviation from the mean value.

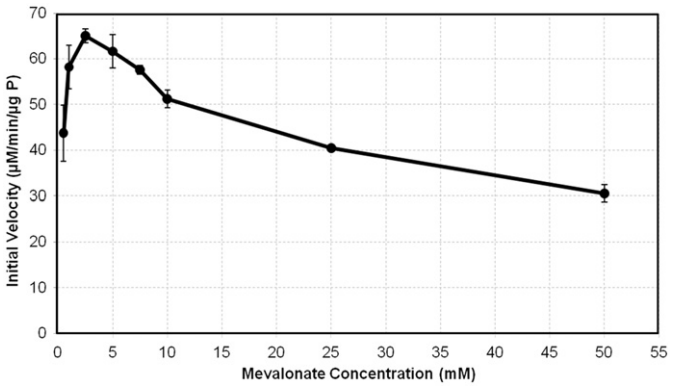

Fig. 6. Substrate inhibition of *S. cerevisiae* mevalonate kinase by mevalonate. Initial reaction velocity as a function of mevalonate concentration. The fastest reaction velocity was measured at 2.5 mM mevalonate. Standard error in reaction velocity for a given mevalonate concentration was determined by triplicate measurements. Higher concentrations of mevalonate correspond to over a 50% reduction in maximal reaction rate.

In re-examining Figs. 4 and 5 it appears all strains exhibit average mevalonate concentrations ranging from 0.7 to 2.8 mM. The range of mevalonate concentrations seen in these experiments suggests that the mevalonate kinase activity may slow down for the strain bearing the *S. aureus* HMGR. To further assess the possibility of substrate inhibition we explored the presence of excess mevalonate in strains engineered for amorphadiene production bearing the HMGRs from *S. aureus* and *D. acidovorans*. GC-MS analysis of the organic extract from aerobic production 48 h post induction with the strain bearing the *S. aureus* HMGR confirmed the presence of unused mevalonate (Fig. S7A), unlike its counterpart bearing the *D. acidovorans* HMGR (Fig. S7B). These data suggest that HMGRs with very high forward reaction rates could have detrimental effects on production levels of the final product. This also opens up the intriguing possibility of improving production levels through appropriate protein engineering of MK if indeed intracellular mevalonate levels reach the inception of suboptimal MK activity. Previous efforts in improving MK expression levels

has been shown to result in increased amorphadiene production (Anthony et al., 2009; Redding-Johanson et al., 2011). If substrate inhibition becomes a predicament, a potential resolution could be found in looking at the mechanism for substrate inhibition by competitive binding inside the active site, as was suggested recently for ferrochelatase (Hunter and Ferreira, 2010). Upon mutation of a single residue near the binding pocket of this enzyme, substrate inhibition was lowered by two orders of magnitude, and a mutation directly inside the binding site eliminated substrate inhibition entirely. This mutation in the binding pocket, while eliminating substrate inhibition, also resulted in disruption of the complex substrate–enzyme interaction resulting in a dramatic reduced ability of ferrochelatase to catalyze at low substrate concentrations, displaying the intricacy of this protein engineering challenge. A similar approach to mutate the allosteric mevalonate binding site of MK could potentially be employed to improve the kinetic behavior of this enzyme. The vital component is to eliminate or shift the threshold MK substrate inhibition point while maintaining its ability to catalyze at low mevalonate concentrations. We postulate that one rationalization of why the *D. acidovorans* HMGR produces more amorphadiene than its counterparts may be partially attributed to its kinetic ability to fine tune the balance between HMG-CoA levels below the cellular toxicity threshold and the mevalonate levels below concentrations that inhibit MK activity.

3.6. Enhancing the NADH pool through the expression of a NADH-regenerating enzyme

From aerobic mevalonate production analysis with the current protein levels, we observed that the HMGRs that required NADH produced less mevalonate than those that required NADPH (Figs. 4 and 5). From *in vitro* studies we discovered that most of these enzymes have the ability to perform the reverse reaction from mevalonate to HMG-CoA. Since we had already employed state-of-the-art sequence optimization techniques to express the HMGR variants in this study, we alternatively focused our efforts on manipulating cofactor levels in the engineered *E. coli* strain. We hypothesized that increasing the availability of reducing equivalents would enhance the forward reaction rate and improve production levels. Given the results seen in Fig. 5, and the vast difference in its *in vitro* forward and reverse reaction rates, we chose to further improve the *in vivo* performance of the *D. acidovorans* HMGR by increasing available intracellular NADH. To this end we introduced an additional enzyme, the NAD^+-dependent formate dehydrogenase from *Candida boidinii,* into the amorphadiene-producing strain bearing the *D. acidovorans* HMGR. The advantage of this system is its independence from perturbation to *E. coli* central metabolism (Heuser et al., 2007; San et al., 2002) and the benefit of increasing the levels of NADH during conversion of formate to carbon dioxide (Berrios-Rivera et al., 2002).

The NADH regeneration scheme was explored via polycistronic expression of FDH in sequence with the amorphadiene synthase gene. Aerobic shake flask experiments were performed as before, but with supplementation of various concentrations of formate (50, 100, 150, and 200 mM) two hours post induction. Successful heterologous expression was confirmed for all proteins in the system by protein quantification (see the section Methods). The results of this host engineering experiment through increased cofactor production are summarized in Fig. 7. Co-expression of FDH alone without addition of exogenous formate resulted in a modest improvement in amorphadiene production (7%) over the strain lacking FDH. *E. coli* produces a minute amount of formate during aerobic fermentation (Berrios-Rivera et al., 2002), thus allowing a slight increase in intracellular NADH by FDH to counterbalance the redox step HMGR catalyzes.

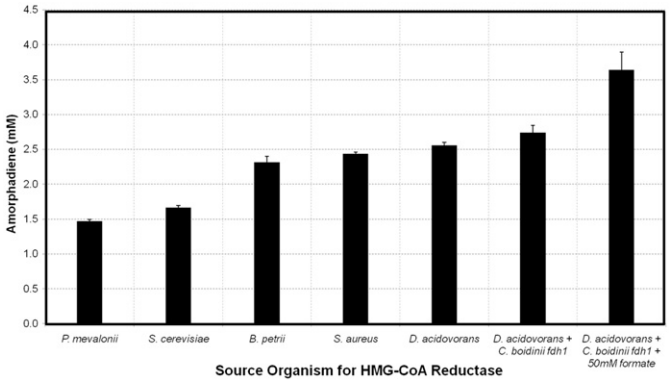

Fig. 7. *In vivo* aerobic production of amorphadiene with synthetic operon 1 expressing various HMGRs, synthetic operon 2, and amorphadiene synthase with or without *fdh1* from *C. biodinii* and 50 mM exogenous formate. Amorphadiene titers were measured as before 48 h after induction. All cultures reached a similar cell density of approximately $OD_{600} \approx 5$. Results are the average of three technical replicates with error bars showing the standard deviation from the mean value.

However, addition of 50 mM formate to the growth medium significantly increased (by 44%) the amorphadiene levels. Provision of exogenous formate displayed sizeable effects not only in amorphadiene production, but also cell growth (data not shown). In the strain lacking FDH, formate supplementation resulted in lower production of amorphadiene and lower overall cell density. In the strain containing FDH, exogenous formate did not affect cell growth or amorphadiene production at concentrations lower than 50 mM. The ramifications of exogenous formate on the system are not unanticipated. High formate concentrations have been shown to exert a detrimental effect on cell growth in the absence of FDH. In the presence of FDH addition of exogenous formate greater than 50 mM leads to a more reduced intracellular environment under aerobic conditions (Berrios-Rivera et al., 2002). Consequently, cellular metabolism tries to compensate for the extra NADH by shifting fermentation metabolites to those that require more moles of NADH, such as ethanol (Leonardo et al., 1993), succinate (Causey et al., 2004), and lactate (Baldoma and Aguilar, 1988; de Graef et al., 1999). At higher formate concentrations, the metabolic burden placed on the cells to not only produce amorphadiene, but also compensate for the extra NADH by turning on the lactate and ethanol pathways in order to achieve redox balance led to reduced amorphadiene production and lower cell density. A potential strategy to restrict carbon flux through reductive fermentative pathways may be to knock out the acetate, ethanol, lactate, and succinate pathways from the *E. coli* genome (Jarboe et al., 2010; Nielsen et al., 2009; Zhang et al., 2011).

4. Conclusions

The performance of a heterologous pathway is dictated by the kinetic properties of its enzymatic components as rendered in the intracellular environment of the foreign host. Variation in these kinetic properties may be achieved either by mutagenic experiments to create the desired attributes of an enzyme or through selection of variant enzymes that already incorporate the characteristics sought. Sequence databases offer multiple variants of a given enzymatic activity to optimize engineered pathways in the host platform (Barthelmes et al., 2007; Chang et al., 2009; Schomburg et al., 2002). Here we studied the optimization of a heterologous mevalonate pathway in *E. coli* by perturbing kinetic properties of a single enzyme, HMGR, which mediates a crucial step in the pathway. Previously, this enzyme has been recognized as deficient, leading to bacteriostatic effects. We identified five HMGR candidates from genome sequences of mesophilic microorganisms and

predicted the enzyme cofactor specificities by analyzing a large number of sequences annotated to possess similar activity. *In vitro* biochemical characterization of these HMGR variants not only confirmed our computational predictions of the cofactor specificities but also revealed widely differing kinetic behavior. We examined mevalonate production capabilities of the HMGR variants under aerobic and anaerobic growth conditions to explore the role of reducing equivalent availability on pathway performance. Given its performance in amorphadiene production and its intriguing *in vitro* and *in vivo* biochemical characteristics, we selected the NADH-dependent HMGR from *D. acidovorans* for further optimization. Regeneration of NADH *in vivo* through heterologous expression of a NAD^+-dependent formate dehydrogenase resulted in a 65% improvement in amorphadiene production compared to that of the strain containing the *S. cerevisiae* tHMGR. Finally, addition of exogenous formate resulted in a 120% improvement in amorphadiene production over the initial system. This improvement is striking considering that the improvement involved a single change in one of the nine components of the natural mevalonate pathway from *S. cerevisiae,* and included the addition of a single enzyme to improve the availability of reducing equivalents in the host cell. Although not addressed in this work, the next steps towards further improvement of isoprenoid production in *E. coli* would be to address additional bottlenecks attributed to production post mevalonate synthesis, as well as economical methods towards increasing intracellular NADH levels. While this study involved the addition of exogenous formate to enhance intracellular NADH levels, and subsequently improve the pathway output by 120%, in developing strains for industrial applications one may apply chromosomal manipulations to improve cofactor levels (Martinez et al., 2008; Wubbolts et al., 1990) without the need for formate addition. A logical extension of the protein engineering work would be to look at mevalonate kinase variants that express better in the host platform, and to find alternative more economical methods towards increasing intracellular concentrations of NADH that do not require exogenous addition of formate. Examination of the kinetic properties in additional pathway components such as phosphomevalonate kinase and phosphomevalonate decarboxylase would also be desirable to determine if these enzymes could be further optimized as well.

Acknowledgments

This work conducted by the Joint BioEnergy Institute was supported by the Office of Science, Office of Biological and Environmental Research, of the US Department of Energy under Contract no. DE-AC02-05CH11231. Purified mevalonate kinase was kindly provided by Amyris Biotechnologies. Special thanks to Mario Ouellet and Xinkai Xie for GC-MS experiments. We would like to thank Nathan Hillson and Harry Beller for helpful comments in improving this manuscript. We would also like thank the following people for helpful discussions during the course of this work: Adrienne McKee, Aindrila Mukhopadhyay, Sung Kuk Lee, Seon Won Kim, Li Feng Lee and Adam Arkin.

Appendix A. Supplementary Material

Supplementary data associated with this article can be found in the online version at doi:10.1016/j.ymben.2011.07.001.

References

Anthony, J.R., Anthony, L.C., Nowroozi, F., Kwon, G., Newman, J.D., Keasling, J.D., 2009. Optimization of the mevalonate-based isoprenoid biosynthetic pathway in *Escherichia coli* for production of the anti-malarial drug precursor amorpha-4,11-diene. Metab. Eng. 11, 13–19.

Bach, T.J., Rogers, D.H., Rudney, H., 1986. Detergent-solubilization, purification, and characterization of membrane-bound 3-hydroxy-3-methylglutaryl-coenzyme A reductase from radish seedlings. Eur. J. Biochem. 154, 103–111.

Baldoma, L., Aguilar, J., 1988. Metabolism of L-fucose and L-rhamnose in *Escherichia coli*: aerobic-anaerobic regulation of L-lactaldehyde dissimilation. J. Bacteriol. 170, 416–421.

Barthelmes, J., Ebeling, C., Chang, A., Schomburg, I., Schomburg, D., 2007. BRENDA, AMENDA and FRENDA: the enzyme information system in 2007. Nucleic Acids Res. 35, D511–D514.

Beach, M.J., Rodwell, V.W., 1989. Cloning, sequencing, and overexpression of mvaA, which encodes *Pseudomonas mevalonii* 3-hydroxy-3-methylglutaryl coenzyme A reductase. Journal of bacteriology 171, 2994–3001.

Bennett, G.N., San, K.-Y., 2009. Engineering *E. coli* central metabolism for enhanced primary metabolite production. In: Lee, S.Y. (Ed.), Systems Biology and Biotechnology of *Escherichia coli*. Springer, Netherlands, pp. 351–376.

Bensch, W.R., Rodwell, V.W., 1970. Purification and properties of 3-hydroxy-3-methylglutaryl coenzyme A reductase from *Pseudomonas*. J. Biol. Chem. 245, 3755–3762.

Berrios-Rivera, S.J., Bennett, G.N., San, K.Y., 2002. Metabolic engineering of *Escherichia coli*: increase of NADH availability by overexpressing an NAD(+)-dependent formate dehydrogenase. Metab. Eng. 4, 217–229.

Berrios-Rivera, S.J., San, K.Y., Bennett, G.N., 2002. The effect of NAPRTase overexpression on the total levels of NAD, the NADH/NAD+ ratio, and the distribution of metabolites in *Escherichia coli*. Metab. Eng. 4, 238–247.

Berry, A., Dodge, T.C., Pepsin, M., Weyler, W., 2002. Application of metabolic engineering to improve both the production and use of biotech indigo. J. Ind. Microbiol. Biotechnol. 28, 127–133.

Bischoff, K.M., Rodwell, V.W., 1992. Biosynthesis and characterization of (S)-and (R)-3-hydroxy-3-methylglutaryl coenzyme A. Biochem. Med. Metab. Biol. 48, 149–158.

Bochar, D.A., Stauffacher, C.V., Rodwell, V.W., 1999. Sequence comparisons reveal two classes of 3-hydroxy-3-methylglutaryl coenzyme A reductase. Mol. Genet. Metab. 66, 122–127.

Boucher, Y., Huber, H., L'Haridon, S., Stetter, K.O., Doolittle, W.F., 2001. Bacterial origin for the isoprenoid biosynthesis enzyme HMG-CoA reductase of the archaeal orders Thermoplasmatales and Archaeoglobales. Mol. Biol. Evol. 18, 1378–1388.

Causey, T.B., Shanmugam, K.T., Yomano, L.P., Ingram, L.O., 2004. Engineering *Escherichia coli* for efficient conversion of glucose to pyruvate. Proc. Natl. Acad. Sci. USA 101, 2235–2240.

Chang, A., Scheer, M., Grote, A., Schomburg, I., Schomburg, D., 2009. BRENDA, AMENDA and FRENDA the enzyme information system: new content and tools in 2009. Nucleic Acids Res. 37, D588–D592.

Chhabra, S.R., Keasling, J.D., 2011. The biological basis | metabolic design and control for production in prokaryotes. In: Moo-Young, Murray (Ed.), Comprehensive Biotechnology, Second Ed., vol. 1. Elsevier, pp. 243–255.

Connolly, D.M., Winkler, M.E., 1989. Genetic and physiological relationships among the *miaA* gene, 2-methylthio-N6-(delta 2-isopentenyl)-adenosine tRNA modification, and spontaneous mutagenesis in *Escherichia coli* K-12. J. Bacteriol. 171, 3233–3246.

de Graef, M.R., Alexeeva, S., Snoep, J.L., Teixeira de Mattos, M.J., 1999. The steady-state internal redox state (NADH/NAD) reflects the external redox state and is correlated with catabolic adaptation in *Escherichia coli*. J. Bacteriol. 181, 2351–2357.

Dueber, J.E., Wu, G.C., Malmirchegini, G.R., Moon, T.S., Petzold, C.J., Ullal, A.V., Prather, K.L., Keasling, J.D., 2009. Synthetic protein scaffolds provide modular control over metabolic flux. Nat. Biotechnol. 27, 753–759.

Edgar, R.C., 2004. MUSCLE: multiple sequence alignment with high accuracy and high throughput. Nucleic Acids Res. 32, 1792–1797.

Fortman, J.L., Chhabra, S., Mukhopadhyay, A., Chou, H., Lee, T.S., Steen, E., Keasling, J.D., 2008. Biofuel alternatives to ethanol: pumping the microbial well. Trends Biotechnol. 26, 375–381.

Gill Jr., J.F., Beach, M.J., Rodwell, V.W., 1985. Mevalonate utilization in *Pseudomonas* sp. *M*. Purification and characterization of an inducible 3-hydroxy-3-methylglutaryl coenzyme A reductase. J. Biol. Chem. 260, 9393–9398.

Glick, B.R., 1995. Metabolic load and heterologous gene expression. Biotechnol. Adv. 13, 247–261.

Harada, H., Misawa, N., 2009. Novel approaches and achievements in biosynthesis of functional isoprenoids in *Escherichia coli*. Appl. Microbiol. Biotechnol. 84, 1021–1031.

Hedl, M., Tabernero, L., Stauffacher, C.V., Rodwell, V.W., 2004. Class II 3-hydroxy-3-methylglutaryl coenzyme A reductases. J. Bacteriol. 186, 1927–1932.

Heuser, F., Schroer, K., Lütz, S., Bringer-Meyer, S., Sahm, H., 2007. Enhancement of the NAD(P)(H) pool in *Escherichia coli* for biotransformation. Engineering in Life Sciences 7, 343–353.

Hunter, G.A., Ferreira, G.C., 2010. Identification and characterization of an inhibitory metal ion-binding site in ferrochelatase. J. Biol. Chem. 285, 41836–41842.

Istvan, E., 2001. Bacterial and mammalian HMG-CoA reductases: related enzymes with distinct architectures. Curr. Opinion Struct. Biol..

Jarboe, L.R., Zhang, X., Wang, X., Moore, J.C., Shanmugam, K.T., Ingram, L.O., 2010. Metabolic engineering for production of biorenewable fuels and chemicals: contributions of synthetic biology. J. Biomed. Biotechnol. 2010, 761042.

Jordan-Starck, T.C., Rodwell, V.W., 1989. *Pseudomonas mevalonii* 3-hydroxy-3-methylglutaryl-CoA reductase. Characterization and chemical modification. J. Biol. Chem. 264, 17913–17918.

Kim, D., Stauffacher, C., Rodwell, V., 2000. Dual coenzyme specificity of *Archaeoglobus fulgidus* HMG-CoA reductase. PRS.

Kuzuyama, T., 2002. Mevalonate and nonmevalonate pathways for the biosynthesis of isoprene units. Biosci. Biotechnol. Biochem. 66, 1619–1627.

Lawrence, C., Chi, Y., Rodwell, V., 1995. Crystallization of HMG-CoA reductase from *Pseudomonas mevalonii*. Acta. Crystallogr. Sect. D: Biol.

Lawrence, C.M., Chi, Y.I., Rodwell, V.W., Stauffacher, C.V., 1995. Crystallization of HMG-CoA reductase from *Pseudomonas mevalonii*. Acta Crystallogr. D Biol. Crystallogr. 51, 386–389.

Leonardo, M.R., Cunningham, P.R., Clark, D.P., 1993. Anaerobic regulation of the *adhE* gene, encoding the fermentative alcohol dehydrogenase of *Escherichia coli*. J. Bacteriol. 175, 870–878.

Leonardo, M.R., Dailly, Y., Clark, D.P., 1996. Role of NAD in regulating the *adhE* gene of *Escherichia coli*. J. Bacteriol. 178, 6013–6018.

Martin, V.J., Pitera, D.J., Withers, S.T., Newman, J.D., Keasling, J.D., 2003. Engineering a mevalonate pathway in *Escherichia coli* for production of terpenoids. Nat. Biotechnol. 21, 796–802.

Martinez, I., Zhu, J., Lin, H., Bennett, G.N., San, K.Y., 2008. Replacing *Escherichia coli* NAD-dependent glyceraldehyde 3-phosphate dehydrogenase (GAPDH) with a NADP-dependent enzyme from *Clostridium acetobutylicum* facilitates NADPH dependent pathways. Metab. Eng. 10, 352–359.

Newman, J.D., Marshall, J., Chang, M., Nowroozi, F., Paradise, E., Pitera, D., Newman, K.L., Keasling, J.D., 2006. High-level production of amorpha-4.11-diene in a two-phase partitioning bioreactor of metabolically engineered *Escherichia coli*. Biotechnol. Bioeng. 95, 684–691.

Nielsen, D.R., Leonard, E., Yoon, S.H., Tseng, H.C., Yuan, C., Prather, K.L., 2009. Engineering alternative butanol production platforms in heterologous bacteria. Metab. Eng. 11, 262–273.

Pfleger, B.F., Pitera, D.J., Smolke, C.D., Keasling, J.D., 2006. Combinatorial engineering of intergenic regions in operons tunes expression of multiple genes. Nat. Biotechnol. 24, 1027–1032.

Pitera, D., Paddon, C., Newman, J., Keasling, J., 2007. Balancing a heterologous mevalonate pathway for improved isoprenoid production in *Escherichia coli*. Metab. Eng.

Redding-Johanson, A.M., Batth, T.S., Chan, R., Krupa, R., Szmidt, H.L., Adams, P.D., Keasling, J.D., Soon Lee, T., Mukhopadhyay, A., Petzold, C.J., 2011. Targeted proteomics for metabolic pathway optimization: application to terpene production. Metab. Eng. 13, 194–203.

Riondet, C., Cachon, R., Waché, Y., Alcaraz, G., Diviès, C., 1997. Measurement of the intracellular pH in *Escherichia coli* with the internally conjugated fluorescent probe 5- and 6-carboxyfluorescein succinimidyl ester. Biotechnol. Tech. 11, 735–738.

Rodwell, V.W., Beach, M.J., Bischoff, K.M., Bochar, D.A., Darnay, B.G., Friesen, J.A., Gill, J.F., Hedl, M., Jordan-Starck, T., Kennelly, P.J., Kim, D.Y., Wang, Y., 2000. 3-Hydroxy-3-methylglutaryl-CoA reductase. Methods Enzymol. 324, 259–280.

San, K.Y., Bennett, G.N., Berrios-Rivera, S.J., Vadali, R.V., Yang, Y.T., Horton, E., Rudolph, F.B., Sariyar, B., Blackwood, K., 2002. Metabolic engineering through cofactor manipulation and its effects on metabolic flux redistribution in *Escherichia coli*. Metab. Eng. 4, 182–192.

Schomburg, I., Chang, A., Schomburg, D., 2002. BRENDA, enzyme data and metabolic information. Nucleic Acids Res. 30, 47–49.

Sherban, D.G., Kennelly, P.J., Brandt, K.G., Rodwell, V.W., 1985. Rat liver 3-hydroxy-3-methylglutaryl-CoA reductase. Catalysis of the reverse reaction and two half-reactions. J. Biol. Chem. 260, 12579–12585.

Takahashi, S., Kuzuyama, T., Seto, H., 1999. Purification, characterization, and cloning of a eubacterial 3-hydroxy-3-methylglutaryl coenzyme A reductase, a key enzyme involved in biosynthesis of terpenoids. J. Bacteriol. 181, 1256–1263.

Theivagt, A.E., Amanti, E.N., Beresford, N.J., Tabernero, L., Friesen, J.A., 2006. Characterization of an HMG-CoA reductase from *Listeria monocytogenes* that exhibits dual coenzyme specificity. Biochemistry 45, 14397–14406.

Voynova, N.E., Rios, S.E., Miziorko, H.M., 2004. *Staphylococcus aureus* mevalonate kinase: isolation and characterization of an enzyme of the isoprenoid biosynthetic pathway. J. Bacteriol. 186, 61–67.

Wilding, E.I., Brown, J.R., Bryant, A.P., Chalker, A.F., Holmes, D.J., Ingraham, K.A., Iordanescu, S., So, C.Y., Rosenberg, M., Gwynn, M.N., 2000. Identification, evolution, and essentiality of the mevalonate pathway for isopentenyl diphosphate biosynthesis in gram-positive cocci. J. Bacteriol. 182, 4319–4327.

Wubbolts, M.G., Terpstra, P., van Beilen, J.B., Kingma, J., Meesters, H.A., Witholt, B., 1990. Variation of cofactor levels in *Escherichia coli*. Sequence analysis and expression of the *pncB* gene encoding nicotinic acid phosphoribosyltransferase. J. Biol. Chem. 265, 17665–17672.

Zhang, W., Li, Y., Tang, Y., 2008. Engineered biosynthesis of bacterial aromatic polyketides in *Escherichia coli*. Proc. Natl. Acad. Sci. USA 105, 20683–20688.

Zhang, X., Wang, X., Shanmugam, K.T., Ingram, L.O., 2011. L-malate production by metabolically engineered *Escherichia coli*. Appl. Environ. Microbiol. 77, 427–434.

Zhu, M.M., Lawman, P.D., Cameron, D.C., 2002. Improving 1,3-propanediol production from glycerol in a metabolically engineered *Escherichia coli* by reducing accumulation of sn-glycerol-3-phosphate. Biotechnol. Prog. 18, 694–699.